Springer

Journal of Mechanical Science and Technology 23 (2009) 1779~1787

Journal of Mechanical Science and Technology

www.springerlink.com/content/1738-494x
DOI 10.1007/s12206-009-0603-1

# Friction-induced ignition modeling of energetic materials †

Min-cheol Gwak, Tae-yong Jung and Jack Jai-ick Yoh*

*School of Mechanical and Aerospace Engineering, Seoul National University, Seoul, Korea 151-742*

(Manuscript Received March 12, 2009; Revised March 27, 2009; Accepted March 28, 2009)

**Abstract**

The heat released during the external frictional motion is a factor responsible for initiating energetic materials under all types of mechanical stimuli including impact, drop, or penetration. We model the friction-induced ignition of cyclotrimethylenetrinitramine (RDX), cyclotetramethylene-tetranitramine (HMX), and ammonium-perchlorate/ hydroxylterminated-polybutadiene (AP/HTPB) propellant using the BAM friction apparatus and one-dimensional time to explosion (ODTX) apparatus whose results are used to validate the friction ignition mechanism and the deflagration kinetics of energetic materials, respectively. A procedure to obtain the time-to-ignition for each energetic sample due to friction is outlined.

*Keywords*: Ignition; Friction; HMX; RDX; AP; HTPB; BAM; ODTX

## 1. Introduction

In many engineering applications, frictional contact occurs between materials and the characterization of contact behavior becomes an important subject of tribology. When two surfaces slide relative to each other, the energy dissipated by the friction becomes the heat source at the interface. The friction intensity is determined by the parameters such as vertical force of load, sliding speed, and material roughness at the contact. A combination of these parameters comprises a basis of flash temperature rise at the contact surface. The surface temperature may give rise to a thermal expansion or chemical oxidation of a testing sample and a variety of physical phenomena of scientific interest. A well established analysis of these phenomena is reported by several researchers in the field [1-3]. Their studies focus on the energy transfer from the contact to the materials by considering a flash or bulk temperature of the surface between the two materials.

Based on the theory of energy transfer in the tribological framework, a study of friction-induced ignition of energetic materials is conducted using simple tests and thermo-chemical and mechanical models for cyclotrimethylenetrinitramine (RDX), cyclotetramethylene-tetranitramine (HMX), and ammonium perchlorate (AP) and hydroxylterminated polybutadiene (HTPB) composite. Gomez *et al*. provided a model to measure the effects of surface heating on ignition in an infinite slab by considering a steady state energy equation with no effect of energetic reactant consumption [4]. In the present model, we consider a set of unsteady equations governing the conservation of energy and the species transport in the energetic sample. Amosov *et al.* developed a simple ignition model of friction, where the amount of heat flux due to friction is a linear function of a contact normal pressure and a sliding velocity [5]. We extend the notion of frictional heat flux as a function of a vertical frictional load and a sliding velocity and utilize the temperature rise at the contact to induce thermal decomposition and runaway reaction of energetic materials.

The experimentally verified global deflagration reaction models of RDX, HMX, and AP/HTPB are first developed before the friction ignition tests are carried out. Then, the BAM test data obtained for each ener-

† This paper was presented at the 7th JSME-KSME Thermal and Fluids Engineering Conference, Sapporo, Japan, October 2008.

*Corresponding author. Tel.: +82 32 872 309682 2 880 9334, Fax.: +82 32 868 171682 2 887 2662
E-mail address: kykim@inha.ac.krjjyoh@snu.ac.kr

getic sample are used to estimate the thermo-friction coefficients for each material whose time-to-ignition at a given load and a velocity is obtained. Since the thermal decomposition process that leads to a thermal runaway can be analyzed through the one-dimensional time to explosion (ODTX) test, the present estimation of time-to-ignition may provide useful information towards enhancing safety and handling of energetic materials at large.

## 2. Model description

In order to describe the thermo-chemical response of energetic materials upon frictional loading, two distinct aspects of present study are identified: first, the chemical reaction of the condensed energetic material is modeled through the thermal decomposition kinetics that has been verified through a series of scaled explosion tests [6, 7]. The second aspect of this work includes the mechanical ignition by friction experiments performed on the BAM apparatus. The applied loading pressure is varied at a specified sliding velocity (7 cm/s) to generate a range of different heat flux conditions at the contact. The calculated time-to-ignition from this test provides useful information when performing sensitivity analysis of energetic materials subject to frictional impact or slide.

### *2.1 Thermal ignition test - One dimensional time to explosion (ODTX)*

The time-to-ignition measurements are made using a standard one-dimensional time to explosion (ODTX) apparatus in which the outer surface of a 1.27 cm diameter energetic sphere is suddenly increased to a specified temperature (see Fig. 1). The time-to-explosion is the time elapsed from the start of heating until confinement failure. The ODTX measurements provide excellent means of validating the thermal explosion kinetics of energetic materials subject to a specified thermal stimulus. Unlike the single-step chemical kinetics of common detonation reactions, the deflagration kinetics with thermal decomposition requires multiple intermediate steps that include solid-solid phase transitions (endothermic) until the final exothermic gaseous reaction leading to a thermal runaway. Fig. 2 illustrates a representative temperature response of energetic material with respect to time for a typical thermal ignition test. The calculated time-to-explosion based on the deflagration model, fitted to the experimental data, captures the general thermal

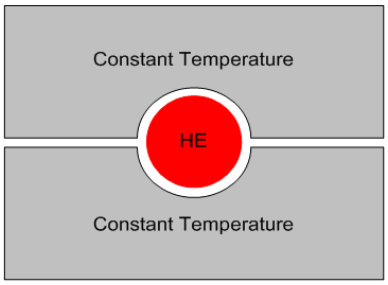


Fig. 1. Schematic of the ODTX apparatus.

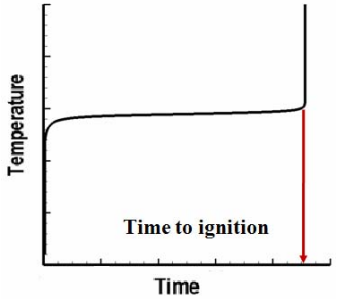


Fig. 2. Modeled thermal (a step) heating of energetic sample until thermal runaway.

runaway phenomena observed from the ODTX apparatus.

### *2.2 Frictional ignition test – BAM friction apparatus*

The friction experimental data are obtained from the Agency for Defense & Development [8] and Los Alamos National Laboratory report [9]. The BAM friction tester is sketched in Fig. 3. The data obtained from the friction tester provide the minimum load by which the sample is ignited within one second at a sliding motion of 7 cm/s. Table 1 summarizes the minimum load required for initiating the energetic samples and the estimated thermo-friction coefficient obtained through the iterative procedure described in this paper. The ignition properties of each sample listed in Table 1 suggest that AP/HTPB propellant has the shortest ignition delay in the friction test. A closer look at each sample's response reveals that the high explosives (HE) namely RDX and HMX response quicker to the lighter load, while the AP/HTPB response is quicker to the heavier load. The fast rate of chemical reaction of high explosives seems to dominate the ignition behavior of test samples, while the thermal diffusion-based initiation is the central mechanism of ignition in the heavier load region. This means that the AP/HTPB propellant is more

Table 1. Calculated thermo-friction coefficients for experimental ignition points.

| | Thermo-friction coefficient $\bar{\mu}$ | Frictional loads measured for ignition at 7 cm/s within 1 second |
|---|---|---|
| RDX | 0.1488 | 16.5 kgf [7, 16] |
| HMX | 0.3226 | 13.6 kgf [7, 16] |
| AP/HTPB | 0.1528 | 11.0 kgf [7] |

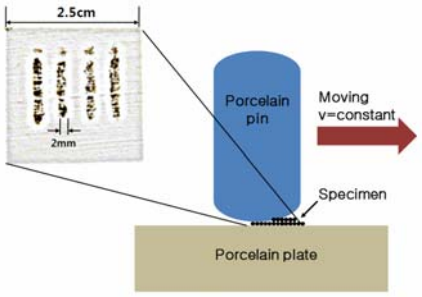


Fig. 3. Schematic of the BAM apparatus at a fixed moving speed, 7 cm/s and variable loading weights.

sensitive to a heavier frictional load greater than 5 kgf, and thus the ignition behavior is consistent with the experimental record of a BAM friction test (see Table 1). More discussions on friction sensitivity of each sample are presented in the following sections.

The time-to-ignition is estimated under a fixed sliding motion of a porcelain pin as a function of load. The correlation of data to a series of physical loading conditions is required in the constructing of a mechanism for friction induced heating and initiation of energetic materials. The basic theory on which we base our analysis is described next.

### *2.3 Analytical description of friction heating*

Two materials under shear motion give rise to a frictional heat rise on contact, which in the present context serves as a site of ignition for the energetic material under consideration. This friction-induced heat is modeled as follows,

$$Q = \bar{\mu} P_n v \tag{1}$$

where $P_n$ is a normal pressure, v is velocity and $\bar{\mu}$ is a thermo-friction coefficient [10-12]. The frictional heat $Q$ is further divided into two parts, reflecting the properties of each contacting materials:

$$Q = Q_1 + Q_2 \tag{2}$$

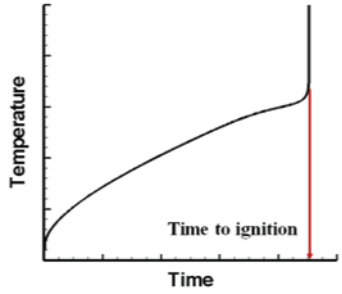


Fig. 4. Modeled frictional heating of energetic sample until thermal runaway.

The ratio of the two heat flux elements is expressed as

$$\frac{Q_1}{Q_2} = \sqrt{\frac{k_1 c_{p,1} \rho_1}{k_2 c_{p,2} \rho_2}} = K_\varepsilon \tag{3}$$

Here $K_\varepsilon$ is the thermal-activity ratio of the contact materials [13], $k$ is thermal conductivity, $c_p$ is heat capacity, and $\rho$ is density. The subscript indices denote each material at contact. From Eqs. (2) and (3), the two fluxes are written as

$$Q_1 = \frac{K_\varepsilon}{1+K_\varepsilon} Q \quad \text{and} \quad Q_2 = \frac{Q}{1+K_\varepsilon} \tag{4}$$

Denoting the energetic sample with subscript 1 and the counterpart surface (a porcelain in the BAM test) with a subscript 2, the overall heat flux due to friction is recovered by summing the two fluxes as in Eq. (2). Shown in Fig. 4 is a typical energetic material response to a frictional load until an ignition is observed.

### *2.4 Thermal transport equation*

#### *2.4.1 Low Peclet number case (1-D)*

The physical problem of interest involves heat generation by friction, heat conduction through the solid energetic materials, and multi-step chemical reactions. The change of frictional load provides vertical push to the energetic sample while the various loading velocities are considered. The assumed motion of friction is slow such that only in the vertical x direction, the thermal diffusion is significant (see Fig. 5). The negligible advective cooling due to a motion $v$ is justified by the ratio of the heat transport due to motion and that due to thermal conduction to be low, that is a low Peclet number ($Pe=vd/k_1$) effect. Here $d$ is width and $k_1$ is thermal conductivity of testing sample. In this

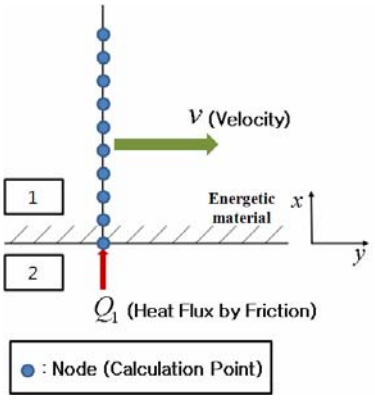


Fig. 5. Schematic of 1-D frictional ignition test of energetic material.

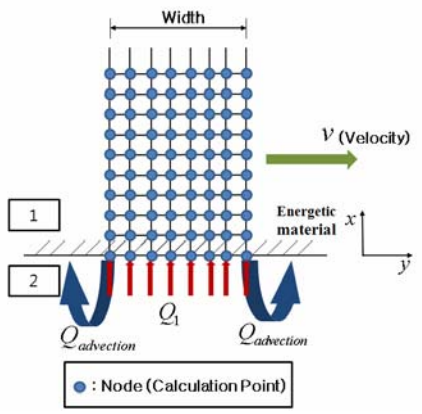


Fig. 6. Schematic of 2-D frictional ignition test of energetic material.

case, the energy conservation requires

$$\rho_1 c_{p,1} \frac{\partial T}{\partial t} = k_1 \frac{\partial^2 T}{\partial x^2} + \sum_{i=1}^{N} r_i q_i \tag{5}$$

where the temperature $T$, the i-th reaction rate $r_i$, heat of reaction $q_i$, and the total number of chemical reaction steps,$N$ are known initially. The species equations are determined by a multi-step deflagration mechanism. A three-step chemical reaction of RDX [6] and a four-step reaction of HMX [7] are used. The two-step deflagration reaction of AP/HTPB similar to those used in [14-16] is developed in this work.

#### *2.4.2 High Peclet number case (2-D)*

If a width, $d$, of constant heat flux along the contact surface between the energetic sample and the porcelain plate moves at a high velocity $v$, the advective heat transfer (a cooling effect, $Q_{advection}$ in Fig. 6) along the surface and two-dimensional thermal diffusion in the sample can be significant. Since the ratio between these two effects, namely advection and diffusion, is reflected through the Peclet number, the strong advection effect can be considered through the following energy balance equation for material 1:

$$\rho_1 c_{p,1} \left( \frac{\partial T}{\partial t} + v \frac{\partial T}{\partial y} \right) = k_1 \left( \frac{\partial^2 T}{\partial x^2} + \frac{\partial^2 T}{\partial y^2} \right) + \sum_{i=1}^{N} r_i q_i \tag{6}$$

As shown in Fig. 6, the semi-infinite body of energetic material moves with a constant speed $v$ along the $y$ axis while the heat source and the related porcelain surface are considered stationary.

### *2.5 Species transport equations*

Regardless of the Peclet number effect, the species transport is governed by the chemical rate laws of deflagration for three energetic materials considered here. The three-step deflagration reaction for RDX is described extensively in [6], and it is recaptured here for clarity:

$$A \rightarrow B, \quad r_1 = Z_1 \exp\left(-E_1 / RT\right) \rho_A \tag{7}$$

$$B \rightarrow C, \quad r_2 = Z_2 \exp\left(-E_2 / RT\right) \rho_B \tag{8}$$

$$C \rightarrow D, \quad r_3 = Z_3 \exp\left(-E_3 / RT\right) \rho^2_C \tag{9}$$

where $A$ and $B$ are solid species, and $C$ and $D$ are intermediate and product gases, respectively. Here, $R$ is a universal gas constant, $Z$ is pre-exponential factor and $E$ is activation energy. The four species transport equations for RDX and a temperature equation are listed below:

$$\rho_1 \frac{\partial Y_A}{\partial t} = -r_1, \quad \rho_1 \frac{\partial Y_B}{\partial t} = r_1 - r_2$$

$$\rho_1 \frac{\partial Y_C}{\partial t} = r_2 - r_3, \quad \rho_1 \frac{\partial Y_D}{\partial t} = r_3 \tag{10}$$

$$\rho_1 c_{p,1} \frac{\partial T}{\partial t} = k_1 \frac{\partial^2 T}{\partial x^2} + q_1 r_1 + q_2 r_2 + q_3 r_3 + \frac{dP_0}{dt} \tag{11}$$

where $Y_i = \rho_i / \rho_1$ is the mass fraction of each component, and $dP_0/dt = 0$ since $P_0$ is constant.

For HMX, the four-step chemical reaction as described in [7] is

$$A \rightarrow B, \quad r_1 = Z_1 \exp\left(-E_1 / RT\right) \rho_A \tag{12}$$

$$B \rightarrow C, \quad r_2 = Z_2 \exp\left(-E_2 / RT\right)\rho_B \tag{13}$$

$$C \rightarrow D, \quad r_3 = Z_3 \exp\left(-E_3 / RT\right)\rho_C \tag{14}$$

$$D \rightarrow E, \quad r_4 = Z_4 \exp\left(-E_4 / RT\right)\rho_D^2 \tag{15}$$

where $A$ and $B$ are solid species, $C$ is solid intermediate, and $D$ and $E$ are final product gases. Then the species transport is governed by the following five equations for HMX and a temperature equation:

$$\rho_1 \frac{\partial Y_A}{\partial t} = -r_1, \qquad \rho_1 \frac{\partial Y_B}{\partial t} = r_1 - r_2,$$
$$\rho_1 \frac{\partial Y_C}{\partial t} = r_2 - r_3, \quad \rho_1 \frac{\partial Y_D}{\partial t} = r_3 - r_4$$
$$\rho_1 \frac{\partial Y_E}{\partial t} = r_4 \tag{16}$$

$$\rho_1 c_{p,1} \frac{\partial T}{\partial t} = k_1 \frac{\partial^2 T}{\partial x^2} + q_1 r_1 + q_2 r_2 + q_3 r_3 + q_4 r_4 + \frac{dP_0}{dt} \tag{17}$$

where $dP_0/dt=0$ as before.

As for the AP/HTPB composite propellant, the following two-step global kinetic scheme is devised, which includes the AP decomposition and one exothermic binder (HTPB) reaction:

$$\text{AP}(A) \rightarrow \text{decomposition products } (B)$$
$$r_1 = Z_1 \exp\left(-E_1 / RT\right)\rho_A P_o^{1.744} \tag{18}$$

$$\beta B + \text{binder}(C) \rightarrow \text{final products}(D)$$
$$r_2 = Z_2 \exp\left(-E_2 / RT\right)\rho_B \rho_C P_o^{1.75} \tag{19}$$

where the rate of reactions suggested by [14] and [16] are modified to fit our ODTX data. The governing equations of thermo-chemical response of AP/HTPB propellant with a mass-based AP/HTPB stoichiometric ratio ($\beta$=88/12, 88% AP and 12% HTPB) are summarized as follows:

$$\rho_1 \frac{dY_A}{dt} = -r_1, \qquad \rho_1 \frac{dY_B}{dt} = r_1 - \beta r_2,$$
$$\rho_1 \frac{dY_C}{dt} = -r_2, \qquad \rho_1 \frac{dY_D}{dt} = r_2(1+\beta) \tag{20}$$

$$\rho_1 c_{p,1} \frac{\partial T}{\partial t} = k_1 \frac{\partial^2 T}{\partial x^2} + q_1 r_1 + q_2 r_2 + \frac{dP_0}{dt} \tag{21}$$

where the ideal equation of state is used for pressure ($P_0(t)=\rho_1 RT(t)$).

For thermal decompositions of RDX, HMX, and AP/HTPB, the species diffusion is insignificant while the thermal conduction is important in forming radicals for accelerating the exothermic chemical reaction to increase the temperature beyond the activation temperature set by the deflagration model. The important thermal condition required at time zero is $T=T_0$, and at the contact boundary $x=0$, a possible flux condition is

$$k_1 \frac{\partial T}{\partial x} = Q_1 \quad \text{at } x = 0 \tag{22}$$

or

$$k_1 \frac{\partial T}{\partial x} - h\left(T - T_0\right) = Q_1 \quad \text{at } x = 0 \tag{23}$$

Here the constant heat flux condition is defined in Eq. (22) while the flux condition in Eq. (23) adds convective heat loss to the surrounding. $h$ is a convection coefficient ($h$=29.8 W/m2K), and the surrounding temperature is 293K [18].

In principle, a total of four test combination is devised in this analysis; i) 1-D model utilizes Eqs. (5) and (22), ii) 1-D + Convection model uses Eq. (5) and (23), iii) 2-D model utilizes Eqs. (6) and (22), and finally iv) 2-D + Convection model solves Eq. (6) and (23). The effects of these different considerations are evaluated in the sections that follow.

## 3. Results

The experimental conditions on the BAM tester are as follows. The contact area is a circle of diameter 2 mm in Fig. 2. This contact area is needed in calculating the loading pressure $P_n$. The thermal-activity ratio of the two contact materials $K_e$ is established with the data listed in Table 2.

Table 2. Material properties of each sample at 300 K.

| | Porcelain | RDX | HMX | AP /HTPB |
|---|---|---|---|---|
| Density (kg/m$^3$) | 2400 | 1820 | 1865 | 1826 |
| Heat capacity (J/kg K) | 897 | 1260 | 1190 | 1255 |
| Thermal conductivity (W/m K) | 2.06 | 0.26 | 0.456 | 0.389 |

### *3.1 Ignition via thermal heating - testing of deflagration kinetics*

The thermo-chemical reaction rate parameters of RDX, HMX, and AP/HTPB are given in Tables 3-5. These parameters have been fitted to the ODTX data to establish accurate deflagration kinetics for each energetic sample tested. For a full description of the basic theory of thermal ignition modeling of RDX and HMX, readers may find the papers [6, 7] informative. On the other hand, the thermal response of AP/HTPB is newly built in this work by utilizing the material data of AP/HTPB composite propellant in Tables 2 and 5. The time-to-explosion for all three energetic materials is shown in Figs. 7-9 with available experimental data which are compared with the present calculation. In these figures, x-axis is the inverse temperature at which the energetic samples are heated (in Fig. 1), and y-axis indicates the time delay at a given temperature until explosion is observed. The ODTX result shows the noted accuracy of modeled response of energetic samples exposed to thermal stimuli. The friction induced ignition of the samples is developed from this accurately tuned deflagration kinetics, as discussed next.

Table 3. Deflagration reaction rate parameters for RDX.

| Reaction step | ln $Z$ ($s^{-1}$) | $E$ (kJ/mol) | Reaction order | Heat of reaction $Q$ (kJ/kg) |
|---|---|---|---|---|
| 1 | 43.7 | 197.2 | 1 | -139 |
| 2 | 38.9 | 184.7 | 1 | +535.6 |
| 3 | 33.15 | 137.8 | 2 | +4780 |

Table 4. Deflagration reaction rate parameters for HMX.

| Reaction step | ln $Z$ ($s^{-1}$) | $E$ (kJ/mol) | Reaction order | Heat of reaction $q$ (kJ/kg) |
|---|---|---|---|---|
| 1 | 48.13 | 202.93 | 1 | -41.88 |
| 2 | 48.7 | 220.64 | 1 | -209.38 |
| 3 | 28.1 | 142.77 | 1 | +808.21 |
| 4 | 32.7 | 161.48 | 2 | +6155.7 |

Table 5. New deflagration reaction rate parameters for AP/HTPB (a mass-based AP/HTPB stoichiometric ratio $\beta$=7.51).

| Reaction step | ln $Z$ ($s^{-1}$) | $E$ (kJ/mol) | Reaction order | Heat of reaction $q$ (kJ/kg) |
|---|---|---|---|---|
| 1 | 7.08 | 124.73 | 1 | -1806 |
| 2 | 9.46 | 149.67 | 2 | +9643.2 |

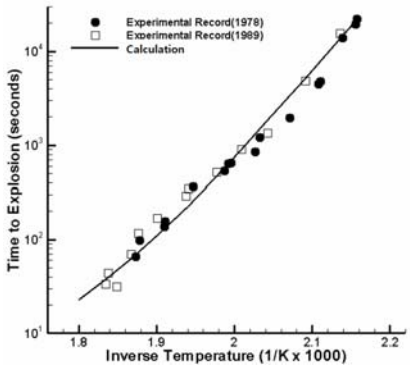


Fig. 7. Calculated thermal ignition curve for 95% HMX 5% Polymer composite sample.

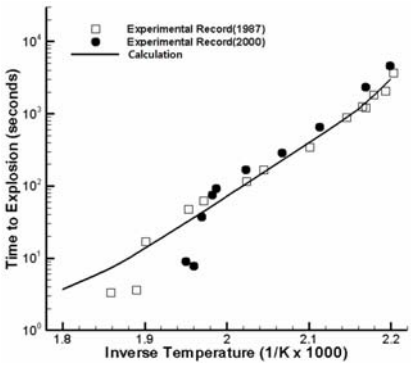


Fig. 8. Calculated thermal ignition curve for 65% RDX 35% binder composite sample.

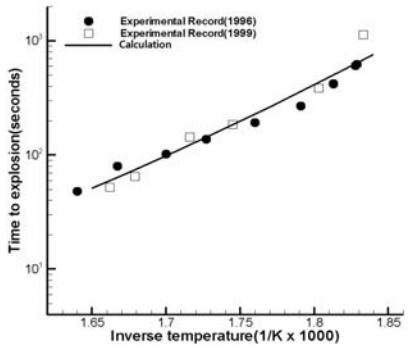


Fig. 9. Calculated thermal ignition curve for AP-HTPB propellant sample.

### *3.2 Ignition via frictional heating*

The thermo-friction coefficient based on a single ignition time is used towards establishing a range of friction ignition conditions of practical interest. For RDX, the thermo-friction coefficient $\bar{\mu}$ is found as 0.1488 through iteratively solving Eqs. (10) and (11)

subject to Eq. (22) or (23) until the experimental time to ignition is obtained. As for the HMX sample, the coefficient is 0.3226 by iteratively solving Eqns. 16 and 17 with a constraint in Eq. (22) or (23) until the experimental time-to-ignition is achieved. We note that the coefficient of HMX is bigger than that of RDX which is consistent with the experimental data [17]. In the case of AP/HTPB, the coefficient is 0.1528 by iteratively solving Eq. (20)-(23).

Figs. 10-12 show calculated times-to-ignition for a range of frictional loads under constant sliding velocity, 7 cm/s. The prediction curve of each sample

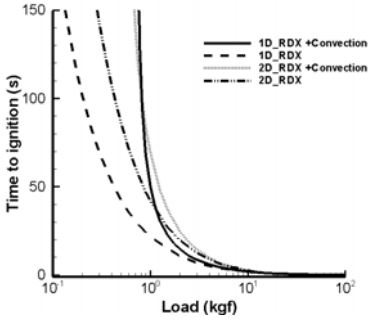


Fig. 10. Calculated frictional ignition curves for pure RDX using four different ignition models.

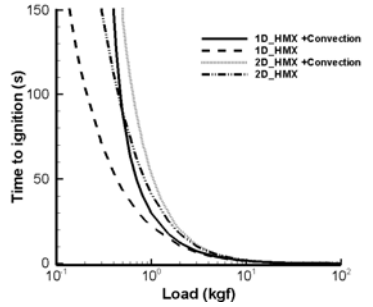


Fig. 11. Calculated frictional ignition curves for pure HMX using four different ignition models.

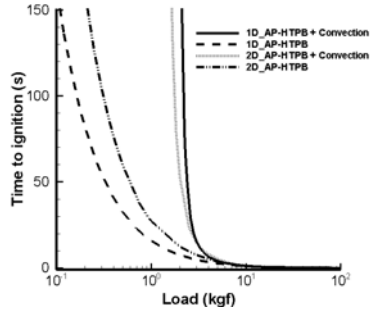


Fig. 12. Calculated frictional ignition curves for AP-HTPB composite propellant using four different ignition models.

serves as a border between the go and no-go regions for friction induced initiation. The convective effect in low Peclet number case is introduced through the boundary condition (Eq. (23)). The same effect in high Peclet number case is implemented through both explicit advection term in Eqn. 6 and the condition in Eq. (23).

Fig. 10 shows the time-to-ignition prediction of RDX. On the right side of the curve, the sample will ignite. For a test load of 16.5 kgf, for example, the friction between the RDX sample and the porcelain pin would trigger ignition at time greater than 1 second. Below 1 second, the same sample falls into no-go region with no ignition. Likewise for HMX, Fig. 11 shows the calculated ignition time corresponding to various loadings. The convection effects in both low and high Peclet number cases seem insignificant in the applied loads above 5 kgf. The frictional property of HMX loaded at 5 kgf or less is shown sensitive to the convective effects. In the lighter region, say below 5 kgf, the convective effect cools the surface of ignition quickly and raises the ignition time to far

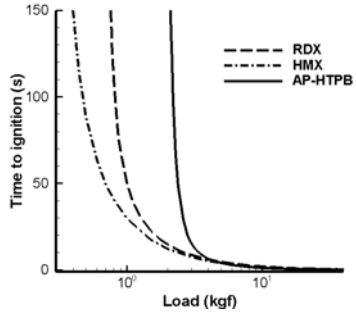


(a) Lighter load region

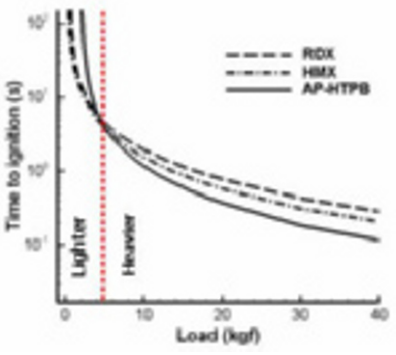


(b) Heavier load region

Fig. 13. Friction ignition curves (shown 1D, Convection) for three samples plotted together for sensitivity comparison. (a) Lighter load region, (b) Heavier load region.

beyond 20 seconds. Similar to high explosive cases, the calculated response of lighter loads of AP/HTPB in Fig. 12 is shown sensitive to the convective effects.

The ignition curves of all three samples plotted together in a single figure can establish overall friction sensitivity of each sample. The 1D+Convection results are used for comparison. Fig. 13 shows that beyond 5 kgf in heavier load region, AP/HTPB is most sensitive to friction while the high explosive samples (RDX and HMX) are more so in the lighter load region. This means that for a lighter testing load below 5 kgf in the test, the effect of heat rise is slow as to delay ignition well beyond the point at which the RDX and the HMX ignite while the AP/HTPB does not. For test loads greater than 5 kgf, the frictional heat flow through conduction is the dominant cause of ignition and the AP/HTPB propellant responded quicker than the less sensitive high explosive samples as verified by the BAM test. The basic findings of this modeling result show potential for providing predictive responses of energetic materials exposed to frictional (or mechanical) stimuli of various kinds.

## 4. Conclusions

We have developed a model for the friction-induced heating and ignition of two high explosives (RDX, HMX) and AP/HTPB rocket propellant. A strategy to define the thermo-friction coefficient for each energetic sample from the experimental data is presented. The three main elements of friction-induced initiation phenomena that include the thermal heat conduction, the deflagration reactions, and the heat flux estimation via the friction mechanism are explained and analyzed by numerical means. Some variations in pressure, temperature conditions and frictional velocities are being considered for future experiments, from which a comprehensive ignition prediction model can be built for studying the energetic materials at large.

## Acknowledgment

Authors would like to thank the generous supports from Brain Korea 21-Phase 2, High Energy Materials Research Center (HM-20), ADD Basic Research (08-08-01), and ADD Grant (0420-20080050) through the SNU Engineering Research Institute and the Institute of Advanced Aerospace Technology. Dr. Ji-Chang Yoo of ADD is warmly acknowledged for providing the friction data.

## References

[1] H. Block, Theoretical study of temperature rise at surfaces of actual contact under oiliness lubrication conditions, *Institution of Mechanical Engineers General Discussion on Lubrication*, 2 (1937) 222-235.

[2] J. C. Jaeger, Moving sources of heat and the temperature at sliding contacts, *Proc. R. Soc, N.S.W*, 76 (1942) 203-224.

[3] J. F. Archard, The temperature of rubbing surfaces, *Wear*, 2 (1958) 438-455.

[4] A. Gomez, G. C. Wake and B. F. Gray, Friction and localized heat initiation of ignition: the asymmetrical slab and cylindrical annulus, *Combustion and Flame,* 61 (1985) 177-187.

[5] A. P. Amosov, S. A. Bostandzhiyan, V. P. Volodin, A. N. Gryadunov and S. M. Muratov, Ignition of a solid explosive by dry friction, *Combustion, Explosion, and Shock Waves*, 14 (1978) 644-648.

[6] J. J. Yoh, M. A. McClelland, J. L. Maienschein, J. F. Wardell and C. M. Tarver, Simulating thermal explosion of cyclotrimethylenetrinitramine-based explosives: Model comparison with experiment, *Journal of Applied Physics*, 97 (2005).

[7] J. J. Yoh and K. H. Kim, Shock compression of condensed matter using Eulerian multimaterial method: Applications to multidimensional shocks, deflagration, detonation and laser ablation, *Journal of Applied Physics*, 103 (2008).

[8] J. C. Yoo, Collection of Material Data on the BAM Test, *Korea Agency for Defense and Development*, 2008.

[9] H. H. Cady, Evaluation of Ferrocyanide / Nitrate Explosive Hazard, *Los Alamos National Laboratory Report*, 1992.

[10] M. F. Ashby, J. Abulawi and H. S. King, Temperature maps for frictional heating in dry sliding, *Tribology Transactions*, 34 (1991) 577-587.

[11] A. D. Randolph, L. E. Hatler and A. Poplato, Rapid heating-to-ignition of high explosives: I. Friction heating, *Ind Eng Chem Fundam*, 15 (1976) 1-6.

[12] Q. Chen and D. Y. Li, A computational study of frictional heating and energy conversion during sliding processes, *Wear*, 259 (2005) 1382-1391.

[13] E. V. Chernenko, L. F. Afanas'eva and N. I. Vaganova, Ignition of powder materials under friction, *Combustion, Explosion, and Shock Waves*, 31

(1995) 635-638.
[14] M. W. Beckstead, R. L. Derr and C. F. Price, A Model of Composite Solid-Propellant Combustion Based on Multiple Flames, *AIAA Journal*, 8 (1970) 2200-2207.
[15] A. Hegab, T. L. Jackson, J. Buckmaster and D. S. Stewart, Nonsteady Burning of Periodic Sandwich Propellants with Complete Coupling between the Solid and Gas Phases, *Combustion and Flame*, 125 (2001) 1055-1070.
[16] X. Zhou, T. L. Jackson and J. Buckmaster, Oscillations in Propellant Flames with Edges, *Combustion and Flame*, 133 (2003) 157-168.
[17] B. M. Dobratz and P. C. Crawford, LLNL Explosive Handbook, *Lawrence Livermore National Laboratory*, 1985.
[18] F. P. Incropera and D. P. Dewitt, Fundamentals of Heat and Mass Transfer 4th edition, *John Wiley & Sons, Inc.*, 1999.

**Min-cheol Gwak** received his B.S. degree in Mechanical Engineering from Korea Aerospace University, Korea, in 2007. Now he is a graduate student of Mechanical and Aerospace Engineering at Seoul National University in Seoul, Korea. His research interests are ignition of high energy material and combustion phenomena.

**Tae-yong Jung** received his B.S. degree in Mechanical and Aerospace Engineering from Seoul National University, Korea, in 2007. Now he is a graduate student of Mechanical and Aerospace Engineering at Seoul National University in Seoul, Korea. His research interests are solid propellant combustion and phase transformation.

**Professor J. Yoh** received his BSME from UC Berkeley in 1992 and MSME from UCLA in 1995. His doctoral degree is in Theoretical & Applied Mechanics from the University of Illinois at Urbana-Champaign, 2001. His research interest is in high energy system design using high power lasers and condensed energetic materials.